

Boundary layer flow of nanofluids over a moving surface in a flowing fluid in the presence of radiation

^aOlanrewaju, P.O., ^bOlanrewaju, M.A. and ^cAdesanya, A.O.

^aDepartment of Mathematics, Covenant University, Ota, Nigeria, West Africa.

^bDepartment of Mechanical Engineering, Cape Peninsula University of Technology, Cape Town, South Africa.

^cDepartment of Mathematics, Landmark University, Omuaran, Nigeria.

Abstract

This study investigates the influence of thermal radiation on boundary layer flow of nanofluids over a moving surface in a flowing fluid. The plate is assumed to move in the same or opposite directions to the free stream. The governing partial differential equations are transformed into ordinary differential equations, a more convenient form for numerical computation, using a similarity transformation. The resulting ordinary differential equations are solved by shooting method alongside with sixth order of Runge-Kutta integration technique. To observe physical insight and interesting aspects of the problem in the presence of thermal radiation, the non-dimensional velocity, temperature and concentration field are numerically studied and displayed graphically for pertinent parameters. It is observed that radiation has dominant effect on the heat transfer and the mass transfer rate. It is further noticed that the heat transfer rate is consistently higher for a nanofluids with smaller value of Le and Pr while the mass flux rate is higher for a nanofluids with higher values of Le and Pr . The results were displayed in tables and in graphs.

Keywords: radiation; Nanofluids; Boundary layer; Moving surface.

1. Introduction

Many industrial processes involve the transfer of heat by means of a flowing fluid in either the laminar or turbulent regime as well as flowing or stagnant boiling fluids. The processes cover a large range of temperatures and pressures. Many of these applications would benefit from a decrease in the thermal resistance of the heat transfer fluids. This situation would lead to smaller heat transfer systems with lower capital cost and improved energy efficiencies. Nanofluids have the potential to reduce such thermal resistances, and the industrial groups that would benefit from such improved heat transfer fluids are quite varied. They include transportation, electronics, medical, food, and manufacturing of many types.

Convective flow in porous media has been widely studied in the recent years due to its wide applications in engineering as postaccidental heat removal in nuclear reactors, solar collectors, drying processes, heat exchangers, geothermal and oil recovery, building construction, etc. (Nield and Bejan [1], Ingham and Pop [2], Vafai [3], Vadasz [4], etc.). It is well known that conventional heat transfer fluids, including oil, water, and ethylene glycol mixture are poor heat transfer fluids, since the thermal conductivity of these fluids plays an important role on the heat transfer coefficient between the heat transfer medium and the heat transfer surface. An innovative technique, which uses a mixture of nanoparticles and the base fluid, was first introduced by Choi [5] in order to develop advanced heat transfer fluids with substantially higher conductivities. The resulting mixture of the base fluid and nanoparticles having unique physical and chemical properties is referred to as a nanofluid. It is expected that the presence of the nanoparticles in the nanofluid increases the thermal conductivity and therefore substantially enhances the heat transfer characteristics of the nanofluid.

Nanofluid is envisioned to describe a fluid in which nanometer-sized particles are suspended in convectional heat transfer basic fluids. Convectional heat transfer fluids, including oil, water, and ethylene glycol mixture are poor heat transfer fluids, since the thermal conductivity of these fluids play important role on the heat transfer coefficient between the heat transfer medium and the heat transfer surface. Therefore numerous methods have been taken to improve the thermal conductivity of these fluids by suspending nano/micro sized particle materials in liquids. There have been published several recent numerical studies on the modelling of natural convection heat transfer in nanofluids: Congedo et al. [6], Ghasemi and Aminossadati [7], Ho et al. [8, 9], etc. These studies have used traditional finite difference and finite volume techniques with the tremendous call on computational resources that these techniques necessitate. A very good collection of the published papers on nanofluids can be found in the book by Das et al. [10] and in the review papers by Wang and Mujumdar [11-13], and Kakaç and Pramuanjaroenkij [14].

Moreover, Oztop and Nada [15] investigated numerical study of natural convection in partially heated rectangular enclosures filled with nanofluids. Furthermore, application of nanofluids for heat transfer enhancement of separated flow encountered in a backward facing step was examined by Nada [16]. Duangthongsuk and Wongwises [17] studied effect of thermophysical properties models on the predicting of the convective heat transfer coefficient for low concentration nanofluid. Ahmad and Pop [18] investigated mixed convection boundary layer flow from a vertical flat plate embedded in a porous medium filled with nanofluids. Boundary layer flow of nanofluids over a moving surface in a flowing fluid was examined by Bachok et al. [19].

In addition to the numerous experimental investigations into nanofluid thermal properties and heat transfer, various investigators have proposed physical mechanisms and mathematical models to describe and predict the phenomena. While comprehensive theoretical models for nanofluids that take all main factors into account are lacking, some progress has been made in this area. Consequently, the classical models and new improvements are presented in this research work by extending the work of Bachok et al. [19] to include the thermal radiation in the energy equation for more physical implications.

2. Mathematical formulation

We consider the steady boundary layer flow of a nanofluid past a moving semi-infinite flat plate in a uniform free stream. It is therefore assumed that the velocity of the uniform stream is U and that of the flat plate is $U_w = \lambda U$, where λ is the plate velocity parameter (see Weidman et al. [21]). The flow takes place at $y \geq 0$, where y is the coordinate measured normal to the moving surface. It is also assumed that at the moving surface, the temperature T and the nanoparticles fraction C take constant values T_w and C_w , respectively, while the values of T and C in the ambient fluid are denoted by T_∞ and C_∞ , respectively. Following the nanofluid model proposed by Tiwari and Das [21] along with the Boussinesq and boundary layer approximations, it is easy to show that the steady boundary layer equations of the present problem are, see also Nield and Bejan [1],

$$\frac{\partial u}{\partial x} + \frac{\partial v}{\partial y} = 0, \quad (1)$$

$$u \frac{\partial u}{\partial x} + v \frac{\partial u}{\partial y} = \nu \frac{\partial^2 u}{\partial y^2}, \quad (2)$$

$$u \frac{\partial T}{\partial x} + v \frac{\partial T}{\partial y} = \alpha \frac{\partial^2 T}{\partial y^2} - \frac{\alpha}{k} \frac{\partial q_r}{\partial y} + \tau \left[D_B \frac{\partial C}{\partial y} \frac{\partial T}{\partial y} + \left(\frac{D_T}{T_\infty} \right) \left(\frac{\partial T}{\partial y} \right)^2 \right], \quad (3)$$

$$u \frac{\partial C}{\partial x} + v \frac{\partial C}{\partial y} = D_B \frac{\partial^2 C}{\partial y^2} + \left(\frac{D_B}{T_\infty} \right) \frac{\partial^2 T}{\partial y^2}, \quad (4)$$

where u and v are the velocity components along the x and y axes, respectively, $\alpha = k/(\rho c)_f$ is the thermal diffusivity of the fluid, ν is the kinematic viscosity coefficient, k is the thermal conductivity, q_r is the heat flux and $\tau = (\rho c)_p / (\rho c)_f$. The boundary conditions Eqs. (1)-(4) are taking to be

$$\begin{aligned} v=0, \quad u=U_w = \lambda U, \quad T=T_w, \quad C=C_w \quad \text{at } y=0, \\ u \rightarrow U, \quad T \rightarrow T_\infty, \quad C \rightarrow C_\infty \quad \text{as } y \rightarrow \infty, \end{aligned} \quad (5)$$

where U is the uniform velocity of the free stream flow. It is worth mentioning that the moving parameter $\lambda > 0$ corresponds to downstream movement of the plate from the origin, while $\lambda < 0$ corresponds to the upstream movement of the plate from the origin. Here we introduce the stream function ψ defined as $u = \partial \psi / \partial x$ and $v = -\partial \psi / \partial y$, which identically satisfies Eq. (1).

The radiative heat flux q_r is described by Roseland approximation such that

$$q_r = -\frac{4\sigma^*}{3K} \frac{\partial T^4}{\partial y}, \quad (6)$$

where σ^* and K are the Stefan-Boltzmann constant and the mean absorption coefficient, respectively. Following Chamkha [20], we assume that the temperature differences within the flow are sufficiently small so that the T^4 can be expressed as a linear function after using Taylor series to expand T^4 about the free stream temperature T_∞ and neglecting higher-order terms. This result is the following approximation:

$$T^4 \approx 4T_\infty^3 T - 3T_\infty^4. \tag{7}$$

Using (6) and (7) in (3), we obtain

$$\frac{\partial q_r}{\partial y} = -\frac{16\sigma^*}{3K} \frac{\partial^2 T^4}{\partial y^2}. \tag{8}$$

Introducing a similarity variable η and a dimensionless stream function $f(\eta)$ and temperature $\theta(\eta)$ as

$$\psi = (2U\upsilon x)^{1/2} f(\eta), \theta(\eta) = \frac{T - T_\infty}{T_w - T_\infty}, \phi(\eta) = \frac{C - C_\infty}{C_w - C_\infty}, \eta = (U/2\upsilon x)^{1/2} y, \tag{9}$$

where prime symbol denotes differentiation with respect to η . Eqs. (2) – (4) reduce to $f''' + ff'' = 0$,

$$\left[1 + \frac{4}{3} Ra\right] \theta'' + Pr f\theta' + Pr Nb\phi'\theta' + Pr Nt\theta'^2 = 0, \tag{11}$$

$$\phi'' + Le f\phi' + \frac{Nt}{Nb} \theta'' = 0, \tag{12}$$

subject to the boundary conditions

$$f(0) = 0, f'(0) = \lambda, \theta(0) = 1, \phi(0) = 1, \tag{13}$$

$$f'(\eta) \rightarrow 1, \theta(\eta) \rightarrow 0, \phi(\eta) \rightarrow 0 \text{ as } \eta \rightarrow \infty,$$

where the five parameters are defined by

$$Ra = \frac{4\alpha\sigma^* T_\infty^3}{kK}, \quad Pr = \frac{\upsilon}{\alpha}, \quad Le = \frac{\upsilon}{D_B}, \tag{14}$$

$$Nb = \frac{(\rho c)_p D_B (\phi_w - \phi_\infty)}{(\rho c)_f \upsilon}, \quad Nt = \frac{(\rho c)_p D_T (T_w - T_\infty)}{(\rho c)_f T_\infty \upsilon}.$$

Here Ra, Pr, Le, Nb and Nt represent the radiation field parameter, Prandtl number, Lewis number, the Brownian motion parameter and the thermophoresis parameter, respectively. We notice that when Ra is zero, it reduces to Bachok et al. [19]. Similarly, when Ra, Nb and Nt are zero, Eqs. (11) and (12) involve just two depend variables, namely $f(\eta)$ and $\theta(\eta)$, and the boundary-value problem for these two variables reduces to the classical problem of Weidman et al. [21] for an impermeable moving surface in a Newtonian fluid.

The quantities of practical interest are the skin-friction coefficient C_f , the local Nusselt number Nu_x and the local Sherwood number Sh_x which are defined as

$$C_f = \frac{\tau_w}{\rho U^2}, \quad Nu_x = \frac{xq_w}{k(T_w - T_\infty)}, \quad Sh_x = \frac{xq_m}{D_B(C_w - C_\infty)}, \tag{15}$$

where τ_w, q_w and q_m are the shear stress, heat flux and mass flux at the surface. Using variables (9), we obtain

$$(2Re_x)^{1/2} = f''(0), \quad \left(\frac{Re_x}{2}\right)^{-1/2} Nu_x = -\theta'(0), \quad \left(\frac{Re_x}{2}\right)^{-1/2} Sh_x = -\phi'(0), \tag{16}$$

where $Re_x = Ux/\upsilon$ is the local Reynolds number. According to Bachok et al. [19], $Re_x^{-1/2} Nu_x$ and $Re_x^{-1/2} Sh_x$ are referred to as the reduced Nusselt number and reduced Sherwood numbers which are represented by $-\theta'(0)$ and $-\phi'(0)$, respectively.

Table 1: Computation showing $f''(0)$, $-\theta'(0)$ and $-\phi'(0)$ for the embedded flow parameters.

Pr	Nb	Nt	Le	Ra	λ	$f''(0)$	$-\theta'(0)$	$-\phi'(0)$
1	0.1	0.1	2	1	0.1	0.462512231335513724	0.353009090654790525	0.600376409340231842
2	0.1	0.1	2	1	0.1	0.462512231335513946	0.443434647935964543	0.562457035585906096
6	0.1	0.1	2	1	0.1	0.462512231335514001	0.593071654079466048	0.489137269031544864
0.71	0.5	0.1	2	1	0.1	0.462512231335513890	0.285737898169713512	0.662096514552980908
0.71	1	0.1	2	1	0.1	0.462512231335513890	0.255035168828560810	0.667739046702424566
0.71	1.5	0.1	2	1	0.1	0.462512231335513890	0.227175684263961896	0.669454527846779168
0.71	0.1	0.5	2	1	0.1	0.462512231335513668	0.295594542768505164	0.450827958779160820
0.71	0.1	1	2	1	0.1	0.462512231335513668	0.323423738988172282	0.447459049864581682
0.71	0.1	1.5	2	1	0.1	0.462512231335513668	0.276043127809399712	0.348137268360352358
0.71	0.1	0.1	10	1	0.1	0.462512231335513779	0.311046090586418744	1.22044716870212766
0.71	0.1	0.1	20	1	0.1	0.462512231335513835	0.310666650574021486	1.62037385931696987
0.71	0.1	0.1	50	1	0.1	0.462512231335514168	0.310302944402533754	2.36541736605274088
0.71	0.1	0.1	2	2	0.1	0.462512231335513779	0.263891001878680864	0.630473442278061902
0.71	0.1	0.1	2	4	0.1	0.462512231335513890	0.213217651902775474	0.644032507451099523
0.71	0.1	0.1	2	1	0.5	0.328741123610356012	0.369403062629324650	0.818385422420432884
0.71	0.1	0.1	2	1	1	0.000000000000000000	0.424127723429936432	1.01624088342316310
0.71	0.1	0.1	2	1	2	-1.01906103740154763	0.509486510429009608	1.32551731302558640

Table 2: Computation showing $-\theta'(0)$ for various values of Pr when Le = 2, Nb = 0.5, Nt = 0.5, Ra = 1.

λ	$-\theta'(0), Pr=2$	$-\theta'(0), Pr=6$	$-\theta'(0), Pr=10$
-0.3	0.047819542380303004	0.003295769230528344	0.000166213406775072
0.1	0.308307030774321422	0.230620414531485934	0.147537150471109990
0.5	0.389793024298875802	0.328584837455264178	0.232262596807346206
1	0.469486852558989698	0.424759629186832410	0.316475009088326264
1.5	0.536323380372475068	0.504897750569688330	0.386491170541982010
2	0.595154149077500528	0.574892398615186040	0.447347764968361150

Table 3: Computation showing $-\phi'(0)$ for various values of Le when Pr = 2, Nb = 0.5, Nt = 0.5, Ra = 1.

λ	$-\phi'(0), Le=2$	$-\phi'(0), Le=6$	$-\phi'(0), Le=10$
-0.3	0.06151543376887638	0.01028416910268342	0.00575132347682167
0.1	0.66238439234778779	1.05777140734819696	1.29560164171625458
0.5	0.85467940844952228	1.51891728615814992	1.94788285321869536
1	1.04106575969379711	1.95545743340004074	2.55431176201018894
1.5	1.19642560998789270	2.31308177016589278	3.04635782851225478
2	1.33263242375462032	2.62304545528352939	3.47063450012585228

3. Results and discussion

The ordinary differential equations (10)-(12) subject to the boundary condition (13) are solved numerically using the symbolic algebra software Maple [22]. Table 1 presents the computation showing the skin-friction coefficient C_f , the reduced Nusselt number Nu and the reduced Sherwood number Sh for various values of embedded parameters. From Table 1, it is understood that the skin-friction and the rate of heat transfer at the plate surface increases with an increase in Prandtl number while the reduced Sherwood number decreases. It is interesting to note that increase in the Brownian motion parameter Nb has no influence on the skin-friction coefficient but the heat transfer rate increases while the mass transfer decreases at the wall plate. Similarly, increase in the thermophoresis parameter Nt has reverse effects on the rate of heat transfer and the mass transfer at the wall plate compared to Brownian parameter. Increasing the Lewis number and the radiation parameter Le, Ra increases the skin-friction and the reduced Sherwood number at the wall plate while it reduces the heat transfer rate at the wall plate for cooling system. It is also interesting to note that increasing parameter λ decreases the skin-friction at the wall plate but bring an increase in the reduced Nusselt and Sherwood number at the wall plate.

Table 2 shows the reduced Nusselt number for various values of Prandtl number Pr with other flow parameters constant and Table 3 shows the reduced Sherwood number for various values of Le. It is seen that the heat transfer rate is consistently higher for a nanofluid with smaller values of Le and Pr, while on the other hand, the mass flux rate is higher for a nanofluid with higher values of Le and Pr. Figure 1 depicts the fluid temperature profile for various values of Prandtl number Pr with other embedded flow parameters fixed. As Prandtl number increases, the temperature at every location in the thermal boundary layer decreases. The effect of Prandtl number on the Nanoparticle fraction profiles. It is interesting to note that the effect is felt far away from the wall plate. Specifically, between $\eta = 0.6$ and 2, the nanoparticle fraction boundary layer thickness increases but from $\eta > 2$, the nanoparticle fraction boundary layer thickness decreases before satisfying the far field boundary conditions asymptotically which support the numerical results obtained. Figures 3 and 4 represent the effect of Brownian motion parameter Nb on the temperature and the nanoparticle volume fraction profiles. Increasing Nb thickens the thermal boundary layer thickness while the reverse is the case for nanoparticle volume fraction profiles. Increasing Lewis number Le resulted to a decrease in nanoparticle volume fraction boundary layer thickness which agrees with Bachok et al. [19] (see figure 8). The effect of λ is seen in figures 9 to 11. Figure 12 depicts the effect of radiation (absorption) parameter on the thermal boundary layer and it is interesting to note that increasing in Ra leads to an increase in the thermal boundary layer thickness a little away from the wall plate. In figure13, it is also seen that as Ra increases the nanoparticle volume fraction decreases away from the wall plate.

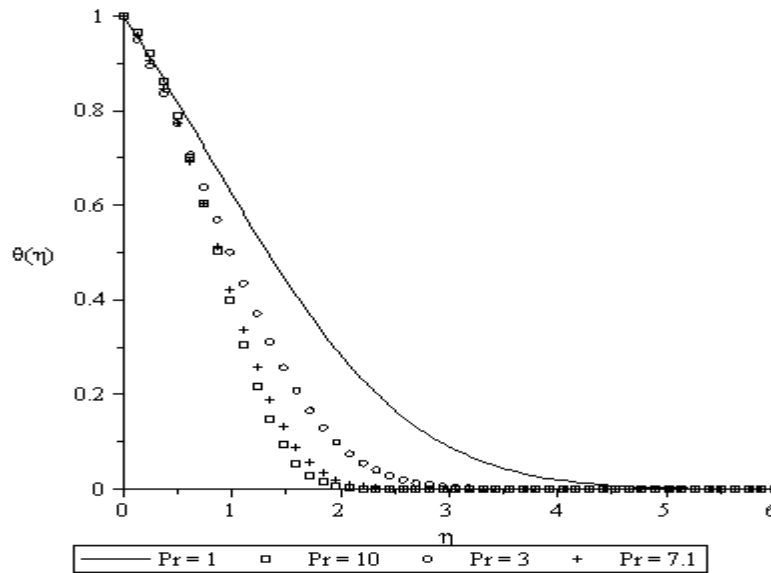


Figure 1: Temperature profiles for various values of Pr when $Nt = 0.5$, $Nb = 0.5$, $Le = 2$, $\lambda = 0.5$, $Ra = 1$.

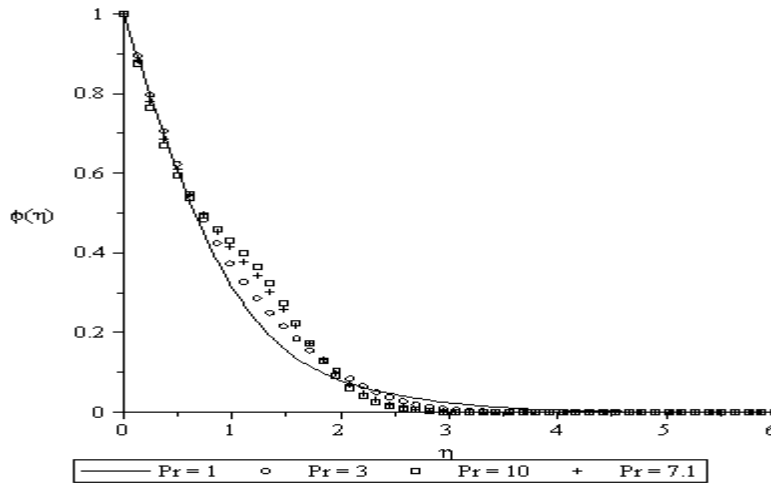


Figure 2: Nanoparticle volume fraction profiles for various values of Pr when $Nt = 0.5$, $Nb = 0.5$, $Le = 2$, $\lambda = 0.5$, $Ra = 1$.

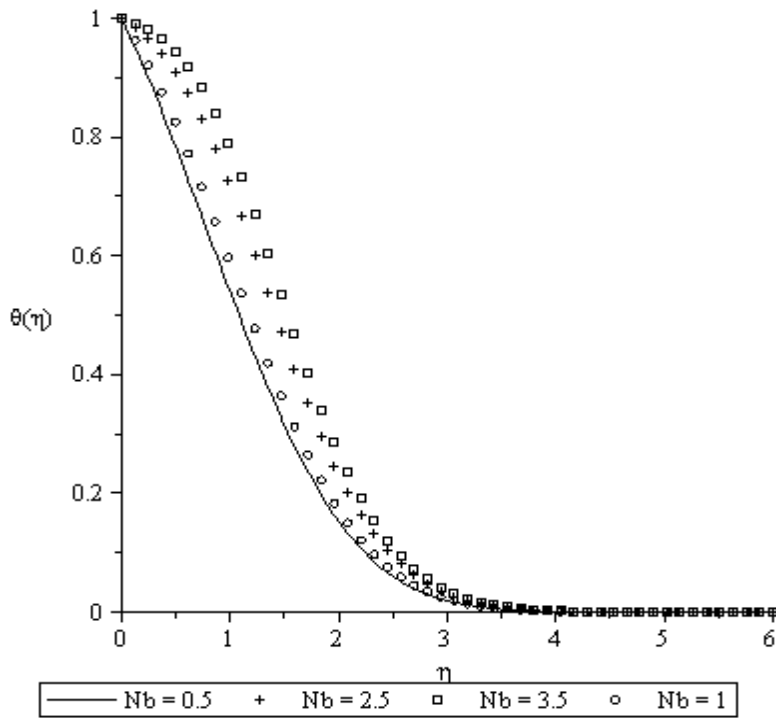


Figure 3: Temperature profiles for various values of Nb when $Nt = 0.5$, $Pr = 2$, $Le = 2$, $\lambda = 0.5$, $Ra = 1$.

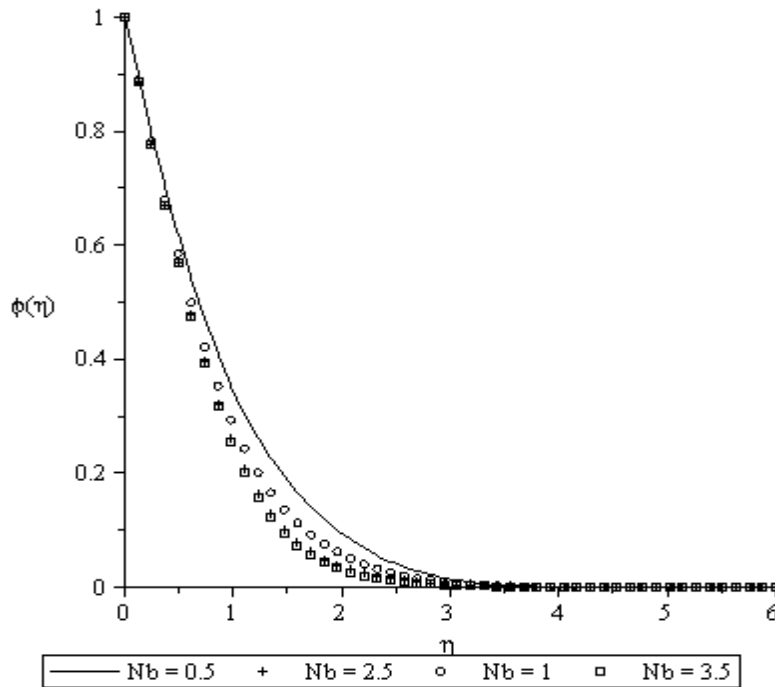


Figure 4: Nanoparticle volume fraction profiles for various values of Nb when $Nt = 0.5$, $Pr = 2$, $Le = 2$, $\lambda = 0.5$, $Ra = 1$.

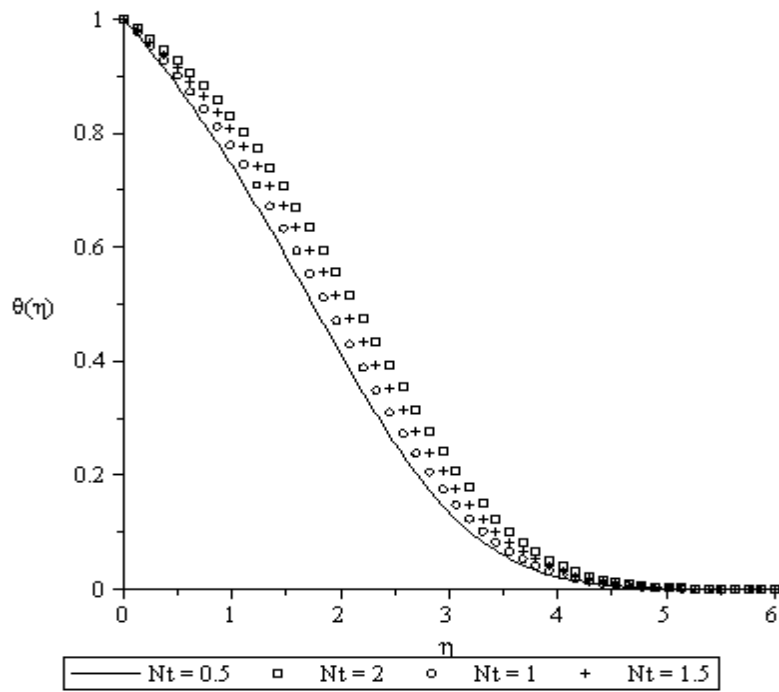


Figure 5: Temperature profiles for various values of Nt when $Pr = 2$, $Le = 2$, $Nb = 2$ and $\lambda = -0.2$.

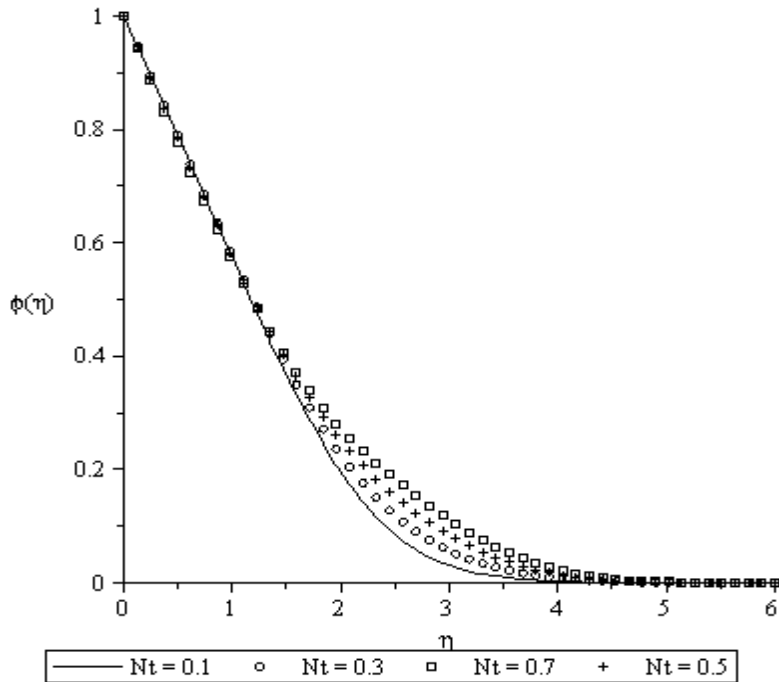


Figure 6: Nanoparticle volume fraction profiles for various values of Nt when $Nb = 0.5$, $Pr = 2$, $Le = 2$, $\lambda = -0.2$, $Ra = 1$.

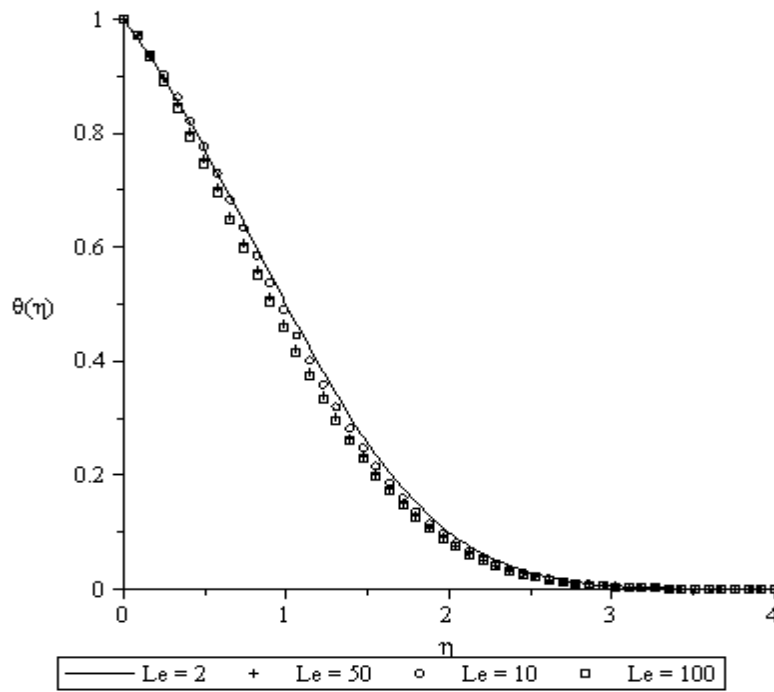


Figure 7: Temperature profiles for various values of Le when $Pr = 2$, $Nt = 0.5$, $Nb = 0.5$, $Ra = 0.5$ and $\lambda = 0.5$.

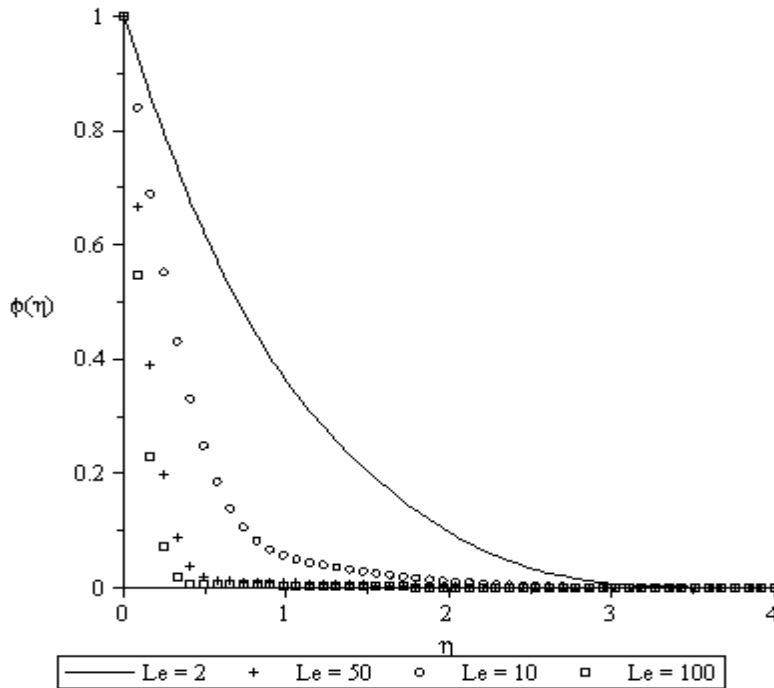


Figure 8: Nanoparticle volume fraction profiles for various values of Le when $Pr = 2$, $Nt = 0.5$, $Nb = 0.5$, $Ra = 0.5$ and $\lambda = 0.5$.

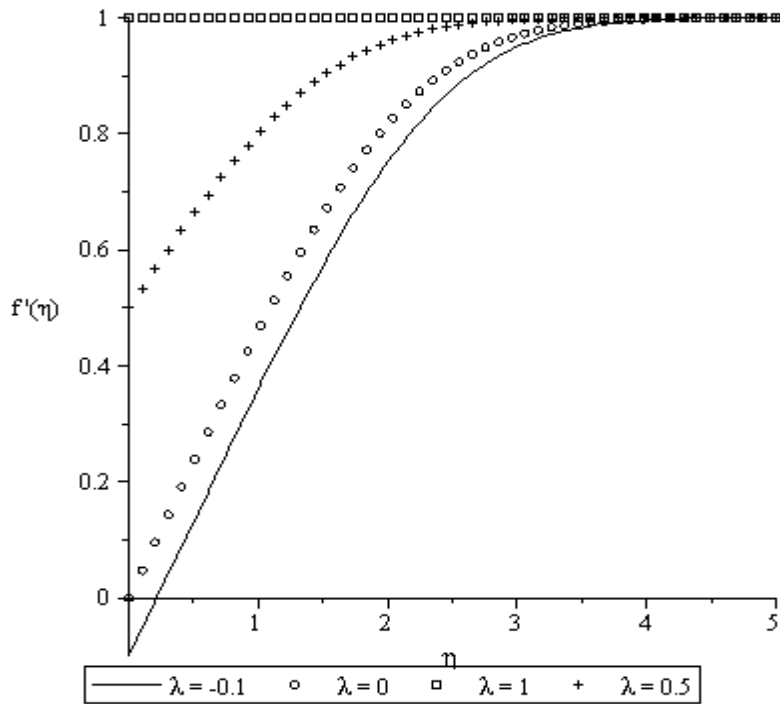


Figure 9: Velocity profiles for various values of λ when $Pr = 2$, $Nt = 0.5$, $Nb = 0.5$, $Ra = 0.5$ and $Le = 2$.

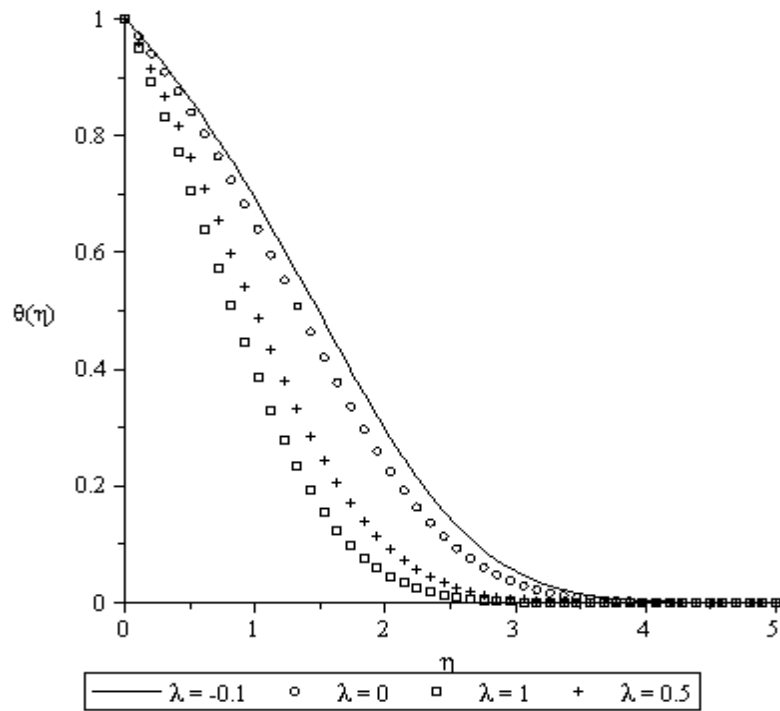


Figure 10: Temperature profiles for various values of λ when $Pr = 2$, $Nt = 0.5$, $Nb = 0.5$, $Ra = 0.5$ and $Le = 2$.

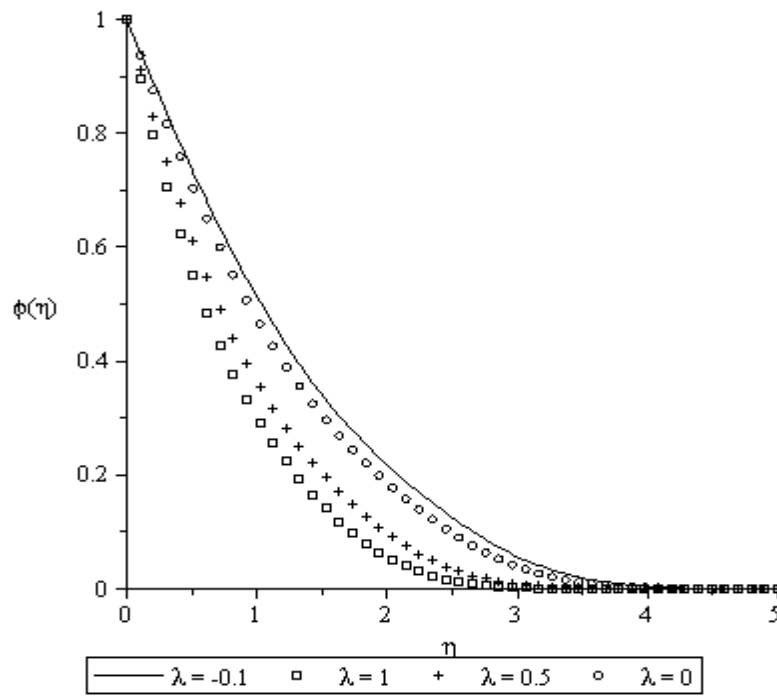


Figure 11: Nanoparticle volume fraction profiles for various values of λ when $Pr = 2$, $Nt = 0.5$, $Nb = 0.5$, $Ra = 0.5$ and $Le = 2$.

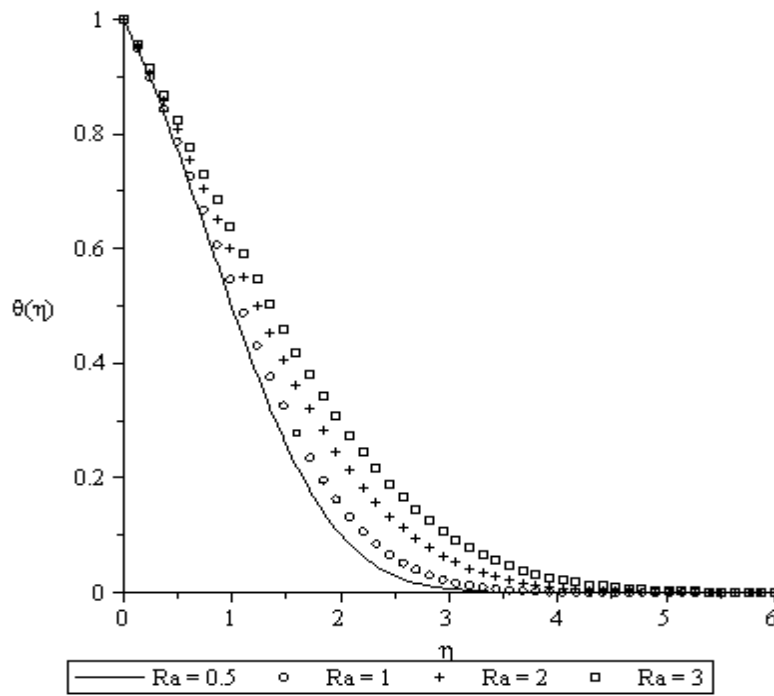


Figure 12: Temperature profiles for various values of Ra when $Pr = 2$, $Nt = 0.5$, $Nb = 0.5$, $\lambda = 0.5$ and $Le = 2$.

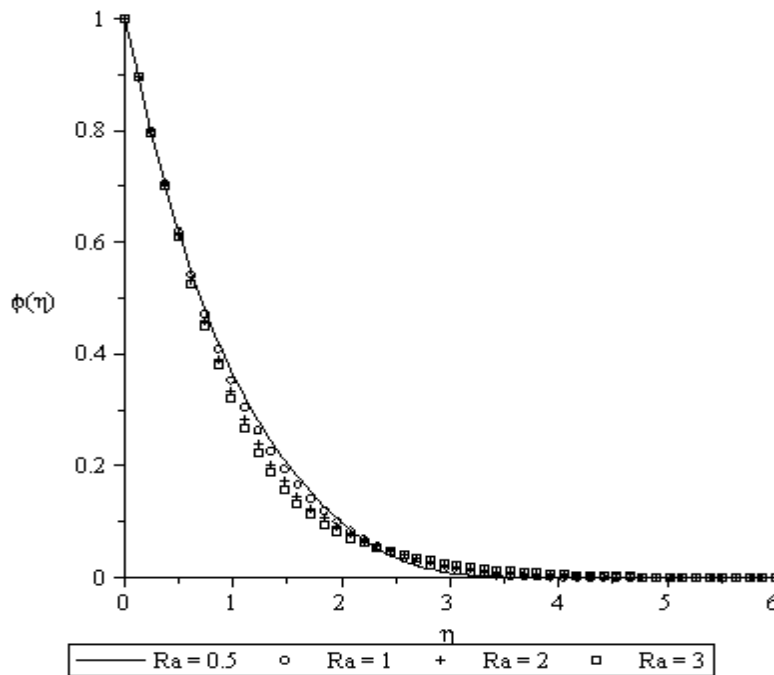


Figure 13: Nanoparticle volume fraction profiles for various values of Ra when $Pr = 2$, $Nt = 0.5$, $Nb = 0.5$, $\lambda = 0.5$ and $Le = 2$.

4. Conclusions

Analysis has been carried out theoretically on the Boundary layer flow of nanofluids over a moving surface in a flowing fluid in the presence of radiation past a moving semi-infinite flat plate in a uniform free stream. A similarity transformation is been used to transformed the governing partial differential equations into ordinary differential equations, a more convenient form for numerical computation. These equations are solved numerically using the shooting method alongside with sixth order of Runge-Kutta integration scheme. Numerical solutions for the skin-friction coefficient, the local Nusselt number and the local Sherwood number as well as for the velocity, temperature and the nanoparticle volume fraction profiles are represented in some graphs for various embedded flow parameter conditions. It was found that radiation has a greater influence on both the thermal boundary layer thickness and the nanoparticle volume fraction profiles and therefore cannot be neglected in engineering applications (electronic cooling).

Acknowledgements

OPO and GJA want to thank Covenant University, Ogun State, Nigeria for their generous financial support.

References

- [1] D.A. Nield, A. Bejan, Convection in Porous Media, third ed., Springer, New York, 2006.
- [2] D.B. Ingham, I. Pop (Eds.), Transport Phenomena in Porous Media, Vol. III, Elsevier, Oxford, 2005.
- [3] K. Vafai (Ed.), Handbook of Porous Media, second ed., Taylor & Francis, New York, 2005.
- [4] P. Vadasz, Emerging Topics in Heat and Mass Transfer in Porous Media, Springer, New York, 2008.
- [5] S.U.S. Choi, Enhancing thermal conductivity of fluids with nanoparticles. ASME Fluids Eng. Division 231 (1995) 99–105.
- [6] P.M. Congedo, S. Collura, P.M. Congedo, Modeling and analysis of natural convection heat transfer in nanofluids. In: Proc. ASME Summer Heat Transfer Conf. 2009, 3 (2009) 569- 579.
- [7] B. Ghasemi, S.M. Aminossadati, Natural convection heat transfer in an inclined enclosure filled with a water-Cuo nanofluid. Numer. Heat Transfer; Part A: Applications, 55 (2009) 807-823.
- [8] C.J. Ho, M.W. Chen, Z.W. Li, Numerical simulation of natural convection of nanofluid in a square enclosure: Effects due to uncertainties of viscosity and thermal conductivity. Int. J. Heat Mss Transfer, 51 (2008) 4506-4516.
- [9] C.J. Ho, M.W. Chen, Z.W. Li, Effect of natural convection heat transfer of nanofluid in an enclosure due to uncertainties of viscosity and thermal conductivity. In. Proc. ASME/JSME Thermal Engng. Summer Heat Transfer Conf. - HT, 1 (2007) 833-841.

- [10] S.K. Das, S.U.S. Choi, W. Yu, T. Pradeep, *Nanofluids: Science and Technology*, Wiley, New Jersey, (2007).
- [11] X.-Q Wang and A.S. Mujumdar, Heat transfer characteristics of nanofluids: a review. *Int. J. Thermal Sci.* 46 (2007) 1-19.
- [12] X.-Q. Wang and A.S. Mujumdar, A review on nanofluids – Part I: theoretical and numerical investigations. *Brazilian J. Chem. Engng.* 25 (2008) 613-630.
- [13] X.-Q. Wang and A.S. Mujumdar, A.S. (2008), A review on nanofluids – Part II: experiments and applications. *Brazilian J. Chem. Engng.* 25 (2008) 631-648.
- [14] S. Kakaç, A. Pramuanjaroenkij, Review of convective heat transfer enhancement with nanofluids. *Int. J. Heat Mass Transfer*, 52 (2009) 3187-3196.
- [15] H.F. Oztop and E. Abu-Nada, Numerical study of natural convection in partially heated rectangular enclosures filled with nanofluids, *International Journal of Heat and Fluid Flow* 29 (2008) 1326-1336.
- [16] E. Abu-Nada, Application of nanofluids for heat transfer enhancement of separated flows encountered in a backward facing step, *International Journal of Heat and Fluid Flow* 29 (2008) 242-249.
- [17] W. Daungthongsuk and S. Wongwises, Effect of thermophysical properties models on the predicting of the convective heat transfer coefficient for low concentration nanofluid, *International Communications in Heat and Mass Transfer* 35 (2008) 1320-1326.
- [18] S. Ahmad and I. Pop, Mixed convection boundary layer flow from a vertical flat plate embedded in a porous medium filled with nanofluids, *International Communications in Heat and Mass Transfer* 37 (2010) 987-991.
- [19] N. Bachok, A. Ishak, I. Pop, Boundary layer flow of nanofluids over a moving surface in a flowing fluid, *International Journal of Thermal Sciences* 49 (2010) 1663-1668.
- [20] A. J. Chamkha (1997). Hydromagnetic natural convection from an isothermal inclined surface adjacent to a thermally stratified porous medium,” *International Journal of Engineering Science*, vol. 37, no. 10-11, pp. 975-986.
- [21] P.D. Weidman, D.G. Kubitschek, A.M.J. Davis, The effect of transpiration on self-similar boundary layer flow over moving surfaces. *Int. J. Eng. Sci.* 44 (2006) 730-737.
- [22] A. Heck, *Introduction to Maple*, 3rd Edition, Springer-Verlag, (2003).